

## Unwrapping 3D complex hollow organs for spatial dose surface analysis

A. Witztum, B. George, S. Warren, M. Partridge, and M. A. Hawkins

Citation: *Medical Physics* **43**, 6009 (2016); doi: 10.1118/1.4964790

View online: <http://dx.doi.org/10.1118/1.4964790>

View Table of Contents: <http://scitation.aip.org/content/aapm/journal/medphys/43/11?ver=pdfcov>

Published by the [American Association of Physicists in Medicine](#)

---

### Articles you may be interested in

[Interindividual registration and dose mapping for voxelwise population analysis of rectal toxicity in prostate cancer radiotherapy](#)

Med. Phys. **43**, 2721 (2016); 10.1118/1.4948501

[A data-mining framework for large scale analysis of dose-outcome relationships in a database of irradiated head and neck cancer patients](#)

Med. Phys. **42**, 4329 (2015); 10.1118/1.4922686

[Spatial and dose-response analysis of fibrotic lung changes after stereotactic body radiation therapy](#)

Med. Phys. **40**, 081712 (2013); 10.1118/1.4813916

[Dosimetric and anatomic indicators of late rectal toxicity after high-dose intensity modulated radiation therapy for prostate cancer](#)

Med. Phys. **35**, 2137 (2008); 10.1118/1.2907707

[Statistical analysis of dose-volume and dose-wall histograms for rectal toxicity following 3D-CRT in prostate cancer](#)

Med. Phys. **32**, 2503 (2005); 10.1118/1.1951427

---



- 3D PATIENT PLAN QA
- 3D IMRT/VMAT PRE-TREATMENT QA
- 3D *IN VIVO* DAILY TREATMENT QA
- ONLINE PATIENT POSITIONING QA

# Unwrapping 3D complex hollow organs for spatial dose surface analysis

A. Witztum,<sup>a)</sup> B. George, S. Warren, M. Partridge, and M. A. Hawkins

CRUK/MRC Oxford Institute for Radiation Oncology, Department of Oncology, University of Oxford, Oxford OX3 7DQ, United Kingdom

(Received 31 May 2016; revised 16 August 2016; accepted for publication 27 September 2016; published 18 October 2016)

**Purpose:** Toxicity dose–response models describe the correlation between dose delivered to an organ and a given toxic endpoint. Duodenal toxicity is a dose limiting factor in the treatment of pancreatic cancer with radiation but the relationship between dose and toxicity in the duodenum is not well understood. While there have been limited studies into duodenal toxicity through investigations of the volume of the organ receiving dose over a specific threshold, both dose-volume and dose-surface histograms lack spatial information about the dose distribution, which may be important in determining normal tissue response. Due to the complex geometry of the duodenum, previous methods for unwrapping tubular organs for spatial modeling of toxicity are insufficient. A geometrically robust method for producing 2D dose surface maps (DSMs), specifically for the duodenum, has been developed and tested in order to characterize the spatial dose distribution.

**Methods:** The organ contour is defined using Delaunay triangulation. The user selects a start and end coordinate in the structure and a path is found by regulating both length and curvature. This path is discretized and rays are cast from each point on the plane normal to the vector between the previous and the next point on the path and the dose at the closest perimeter point recorded. These angular perimeter slices are “unwrapped” from the edge distal to the pancreas to ensure the high dose region (proximal to the tumor) falls in the centre of the dose map. Gamma analysis is used to quantify the robustness of this method and the effect of overlapping planes.

**Results:** This method was used to extract DSMs for 15 duodena, with one esophagus case to illustrate the application to simpler geometries. Visual comparison indicates that a  $30 \times 30$  map provides sufficient resolution to view gross spatial features of interest. A lookup table is created to store the area ( $\text{cm}^2$ ) represented by each pixel in the DSMs in order to allow spatial descriptors in absolute size. The method described in this paper is robust, requires minimal human interaction, has been shown to be generalizable to simpler geometries, and uses readily available commercial software. The difference seen in DSMs due to overlapping planes is large and justifies the need for a solution that removes such planes.

**Conclusions:** This is the first time 2D dose surface maps have been produced for the duodenum and provide spatial dose distribution information which can be explored to create models that may improve toxicity prediction in treatments for locally advanced pancreatic cancer. © 2016 Author(s). All article content, except where otherwise noted, is licensed under a Creative Commons Attribution (CC BY) license (<http://creativecommons.org/licenses/by/4.0/>). [<http://dx.doi.org/10.1118/1.4964790>]

Key words: radiotherapy, dose-surface map, organ unwrapping, toxicity predictors, duodenal toxicity

## 1. INTRODUCTION

Pancreatic cancer is the fifth most common cause of cancer death in the UK, but the five- and ten-year survival rates have only slightly improved since the early 1970s; the overall five-year survival is still less than a bleak 5%.<sup>1</sup> In locally advanced pancreatic cancer (LAPC), seen at diagnosis in around 30% of pancreatic cancer patients,<sup>2</sup> local failure is still a major problem<sup>3–5</sup> with local tumor progression being reported in 25%–62% of patients.<sup>5</sup> It is thought that better local control can be achieved by escalating the dose to the pancreas but duodenal toxicity has proven to be a major dose limiting factor for these efforts.<sup>6–11</sup> To better understand this normal tissue toxicity, it is important to model the relationship between the dose delivered to the organ and the resulting complication.

Previous studies that seek to relate dose to the duodenum to toxicity have reported various statistically significant metrics. Cattaneo *et al.*<sup>12</sup> report that it is the volume of the duodenum receiving more than 40 or 45 Gy that is correlated to GI toxicity grade  $\geq 2$  whereas Kelly *et al.*<sup>5</sup> conclude that it is the volume receiving more than 55 Gy. When considering grade  $\geq 3$  GI toxicity, Huang *et al.*<sup>13</sup> found correlation with the volume of the duodenum receiving more than between 20 and 35 Gy and Nakamura *et al.*<sup>14</sup> found correlation between upper GI bleeding and the volume of the stomach and duodenum receiving more than 50 Gy. These studies are summarized in Table I.

Dose-volume histograms (DVHs) are a standard tool in radiotherapy treatment planning to ensure target coverage and normal tissue sparing. DVHs provide statistical information on the dose distribution within a volume of interest (VOI)

TABLE I. Summary of some studies correlating dose-volume metrics to duodenal toxicity.

Authors	Toxicity	Metric
Cattaneo <i>et al.</i>	GI toxicity grade $\geq 2$	Duodenum V40, V45
Kelly <i>et al.</i>	GI toxicity grade $\geq 2$	Duodenum V55
Huang <i>et al.</i>	GI toxicity grade $\geq 3$	Duodenum V20-35
Nakamura <i>et al.</i>	Upper GI bleeding	Stomach + Duodenum V50

but this reduces a 3D dose distribution to a 1D histogram. It also assumes that the entire VOI is equally important and this is unlikely to be the case for all organs. For hollow organs, such as the rectum, it has been suggested that dose-surface histograms (DSHs) can provide more useful information in understanding tissue response<sup>15–17</sup> although clinically DVHs are still almost universally used for all organs at risk (OARs). For example the QUANTEC review, which does not separate the duodenum from the rest of the small bowel, recommends the absolute volume of small bowel receiving more than 15 Gy should be limited to 120 cm<sup>3</sup> (if delineating bowel loops) for nonSBRT treatments.<sup>18</sup>

Both DVHs and DSHs are still crucially missing spatial information about the dose distribution. For hollow organs, it is likely the spatial distribution such as longitudinal and circumferential distribution will be relevant for dose tolerance. Additionally, having the spatial distribution can also aid in searching for mechanistic explanations of toxicity. It has been demonstrated in studies of the rectum<sup>19,20</sup> that the spatial features in the dose distribution can be useful in predicting toxicity in normal tissue. This information can be preserved in hollow organs by building a 2D DSM. These DSMs can be interpreted in various ways in order to extract information about toxicity. Average DSMs for patients with and without toxicity can be analyzed,<sup>19</sup> as can lateral and longitudinal extent,<sup>20,21</sup> and percentage of circumference receiving more than some dose threshold.<sup>21</sup> DSMs can also be used as inputs for a classification method based on neural networks.<sup>22</sup>

In order to build a 2D DSM from a 3D tubular organ, it is necessary to “unwrap” the 3D structure. This has been done previously on structures with simple geometries, such as the esophagus and rectum.<sup>21,23,24</sup> Munbodh *et al.*<sup>19</sup> unwrap the rectum using a conformal mapping procedure<sup>25</sup> originally used for virtual colonography. Hoogeman *et al.*<sup>23</sup> find the central axis of the rectum using the approximate minimum distance field approach and then create orthogonal cross-sections as described by Zhou *et al.*<sup>21</sup> for the esophagus and the rectum. Buettner *et al.*<sup>20,22</sup> generate DSMs for the rectum slice-by-slice in a similar fashion to Tucker *et al.*,<sup>26</sup> moving through the structure in the superior-inferior (SI) direction and creating planes which model the perimeter. In this paper, simple organs refer to those where it is possible to move through the organ considering each CT transaxial plane as independent. This is not possible when considering geometrically complex organs such as the duodenum as seen in Fig. 1.

While this problem is new in the field of dose surface map creation, it has been seen in the field of virtual colonography. The aim of virtual colonography is surface visualization of

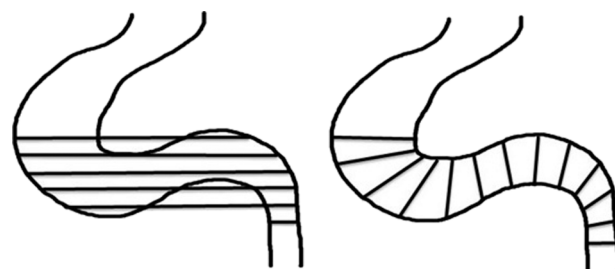


FIG. 1. Left: CT axis slices through the duodenum would not represent a physically meaningful spatial dose. Right: A new axis is required for slices in the duodenum to represent a physically meaningful spatial dose.

the colon and virtual colon navigation in order to aid polyp detection. Therefore the methodologies developed for these goals may not best suit the requirements for dose-surface map creation. One way the shared problem of sampling a surface in an area of high curvature was tackled in virtual colonography was by casting nonlinear rays from the centre line.<sup>27,28</sup> The methods used to curve the rays, such as using electric fields in Wang *et al.*,<sup>28</sup> give a high resolution of the surface but are computationally expensive and such surface detail is not necessarily required in the case where the dose to a single surface point is desired.

In this paper, a new method is presented to simply and meaningfully unwrap the 3D surface dose to a 2D dose-surface map in an effort to preserve the spatial distribution of the dose. The addition of spatial dose information to better understand the relationship between the spatial distribution of dose and duodenal toxicity could play a crucial role in future escalation studies and lead to improved local control in LAPC radiotherapy treatments. This method is also generalizable to other hollow organs.

## 2. MATERIALS AND METHODS

### 2.A. Unwrapping 3D complex hollow organs

The methodology described requires the definition of a new axis, a set of nonoverlapping slices which sample the organ, determination of the dose at the perimeter of these slices, and the ability to extract spatial information from the dose-surface maps in terms of absolute area (cm<sup>2</sup>).

Figure 1 shows that considering transaxial CT slices can result in a single slice containing segments from two different parts of the duodenum. Therefore, a new axis is defined which creates slices oriented normal to a curved line through the organ.

The creation of overlapping slices should be avoided. This is especially key in areas of high curvature where it would result in a spatially meaningless dose distribution. Overlap occurs due to poor definition of the central axis, from which the plane is defined. If a simple geometric central axis is used, as in work with organs such as the rectum and esophagus, the overlap problem remains. A new definition of the central axis which considers the curvature of the duodenum can greatly reduce the problem of overlapping planes. To completely remove any overlap, a further automated step to create nonoverlapping polygons is described.

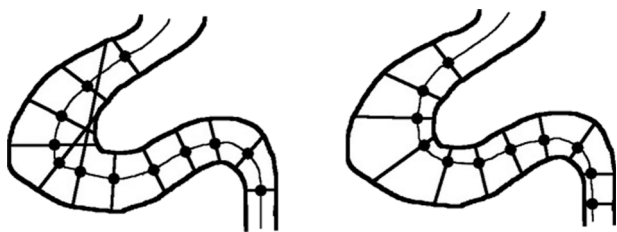


FIG. 2. The need for human visual spline selection is shown. Left: Using the central axis leads to overlapping planes. Right: Using spline points near the edge of high curvature can avoid creating overlapping planes.

The complete methodology can be summarily split into four sections, as follows.

### 2.A.1. Image definition

The contours of the organ of interest and associated dose distribution were exported in DICOM format from an ECLIPSE (v10.0.28, Varian, Palo Alto, CA) treatment planning system to MATLAB (R2014b, The MathWorks, Inc., Natick, MA) using the computational environment for radiotherapy research (CERR).<sup>29</sup> The surface of the organ is defined by finding the alpha shape of the 3D point cloud of the contour using Delaunay triangulation. An alpha shape can be thought of as the resulting volume when a sphere of radius  $r$  is rolled around the point cloud. By setting  $r$  to be greater than the CT slice thickness, the alpha shape defines the volume of the structure.

### 2.A.2. Racecar path

A new central axis is defined to ensure that slices through the organ do not overlap in regions of high curvature. A more desirable path than the geometric central axis is one that moves close to the edges of high curvature, similar to a path favored by a racecar through a track (Fig. 2) but in 3D. A user selects a start and end point in the organ and a path between these points is found considering both length and curvature based on the method described in Ref. 30, which demonstrates the possibility of incorporating higher-order regularization such as curvature to shortest path problems. The path through the organ regulates both length and curvature, with a weighting of 1:10 in this case, to produce the desired racecar path. A spline is fit to the points on this racecar path using Hobby's

algorithm.<sup>31</sup> The spline is discretized to 200 equally spaced points which defines the new central axis spline (CAS). An example CAS from a clinical patient is seen in Fig. 3.

### 2.A.3. Ray casting

Orthogonal planes are created at each CAS point with a normal defined as the vector between the previous and the next point. The surface dose for each plan is found using a two step process. First, eight rays ( $45^\circ$  apart) are cast radially outward on these planes from the CAS point toward the surface. The centroid of these surface points approximates the center of the organ in each plane and is set as the new centers. This is done in order to more uniformly sample the surface points in the second step. Next, moving radially outward from the new center on each plane, 30 rays ( $12^\circ$  apart) are cast toward the surface. Once the ray reaches the surface, the dose is recorded. The final position and associated dose of the 30 rays together make up an angular slice for each CAS point. An example is shown in Fig. 4 with five CAS points used to create angular slices.

If there are overlapping slices, a fixed start and end slice on either side of the overlapping planes is defined [highlighted in black in Fig. 5(a)], as is the number of slices that overlap in between ( $n = 2$  in Fig. 5). Each fixed slice is a 30 edged polygon (triacontagon) on a plane and the vertices of these two polygons are connected [shown in Fig. 5(b)]. These connecting lines are split into the number of slices required between the start and end slices ( $n = 2$  in Fig. 5) and the resulting triacontagons represent the nonoverlapping polygons [shown in red in Figs. 5(c) and 5(d)] which replace the overlapping slices from the original selection. These nonoverlapping polygons may not lie on a single plane but they do meaningfully represent the surface between the two fixed slices.

### 2.A.4. Unwrapping

In the case of the duodenum, an unwrapping marker is defined as the centroid of the PTV. The perimeter point that is closest to the centroid on each angular slice is placed in the middle of the dose map, ensuring the "cutting" of the duodenum takes place on the side distal to the pancreas and the tumor (Fig. 6). For other structures, an unwrapping point or side must be decided. Since the angular slices sample the

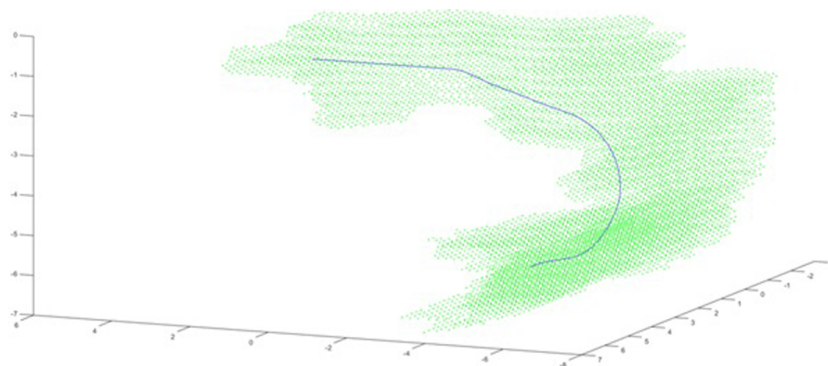


FIG. 3. The "racecar" path found between a user-defined start and end point in a duodenum point cloud.



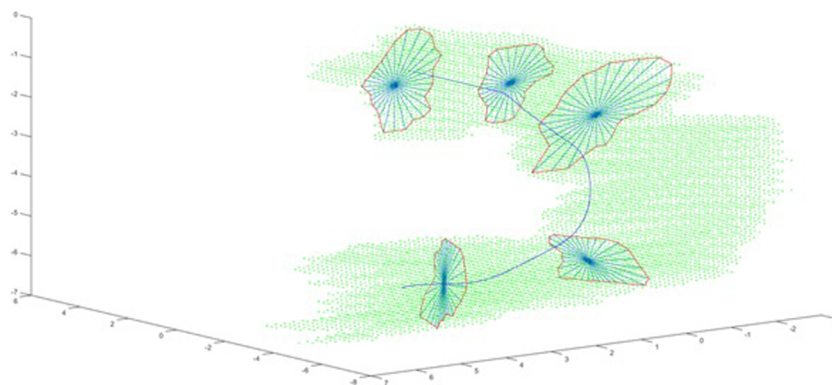


FIG. 4. An example of five out of 30 angular slices from the adjusted center point on the racecar path. The 30 rays cast from the center to the surface are shown. The surface points are connected in red for visual representation of the resulting polygons. (See color online version.)

inner and outer edges differently, a lookup grid is also saved defining the size of each point on the 2D DSM to enable conversion from number of pixels back to absolute volume.

## 2.B. Method robustness

The robustness to spatial sampling errors due to overlapping planes was investigated. Gamma analysis<sup>32</sup> was used to compare the dose maps produced as it is already widely used to compare dose distributions in radiotherapy. Gamma analysis was chosen over dose difference histograms because it is not critical if two similar points are in the exact same place on the dose map. Because we are interested in extracting spatial features gamma analysis does not penalize similar points if

they are close to each other in both maps. While in this case for gamma analysis the dose difference criterion remains as a percentage, the distance to agreement is adjusted to represent number of pixels (from the  $30 \times 30$  grid) rather than an absolute difference. We have accepted gamma at the 3%/3 px level as 95% for the purpose of this work.

### 2.B.1. Slice selection robustness

Only 30 slices are used to describe the final DSM from the discretized CAS points. The process for selecting these slices, including whether or not this process results in slice overlap, was studied and the effect on the resultant dose-surface map quantified.

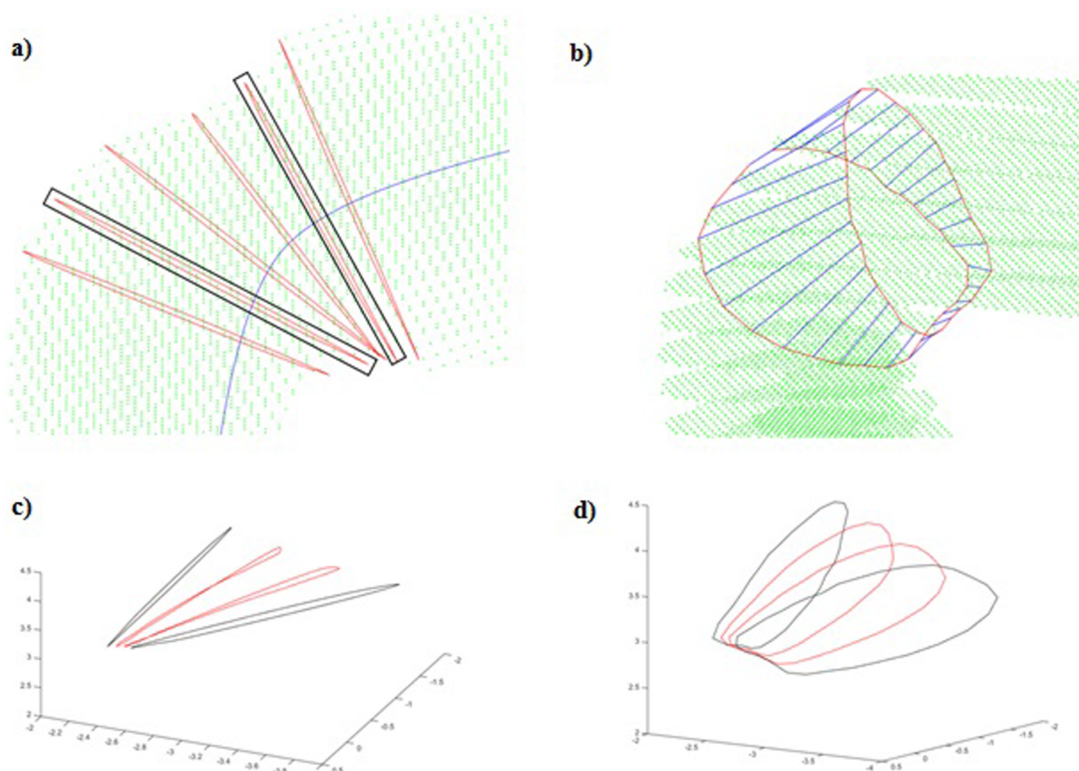


FIG. 5. (a) The two central slices overlap. The two nonoverlapping slices either side are highlighted in black and set as the fixed start and end slices. (b) The 30 vertices of the fixed polygons are connected and the lines between them (in blue) are split into the number of required slices (in this case two slices need to be replaced). [(c) and (d)] Two views of the resulting nonflat polygons (in red) created between the two flat polygons (in black). (See color online version.)

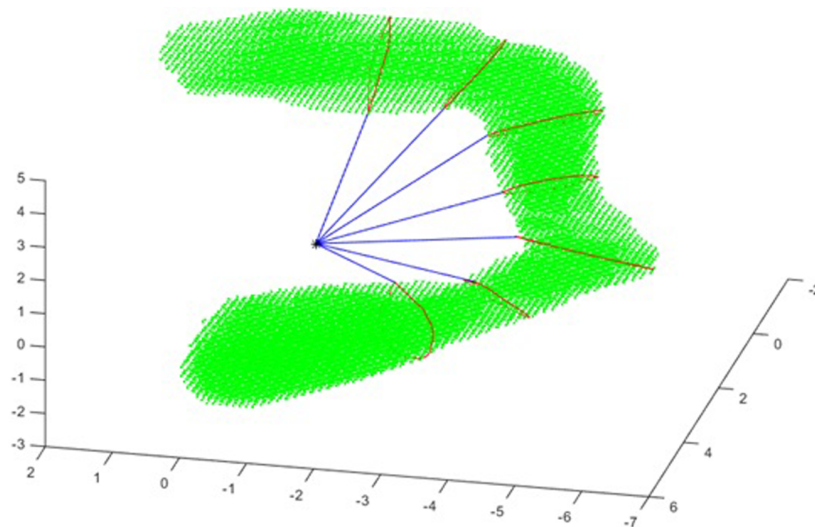


FIG. 6. The point on each angular slice closest to the centroid of the PTV is placed on the middle of the dose map.

### 2.B.2. Overlap fix (polygon) robustness

This method has a built-in step which removes any overlapping slices that remain after selecting a central axis spline (Fig. 5). Each slice is a planar (flat) 30 sided polygon and this method replaces overlapping slices with 30 sided nonplanar polygons which uniformly sample the space previously sampled by these overlapping slices. The effect of using 30 sided nonplanar polygons instead of planar polygons on the dose-surface map was studied.

## 3. RESULTS

### 3.A. Dose-surface maps

The new method described in Sec. 2 was successfully used to unwrap 15 duodena from the ARCII clinical trial (Fig. 7).

Each panel in Fig. 7 represents the DSM for a duodenum for a specific patient. The duodenum was contoured according to RTOG guidelines and reviewed by a radiologist. An esophagus from a lung cancer treatment (with a prescription of 60 Gy in 30 fractions to the planning target volume) was also unwrapped to show the generalizability of this method (Fig. 8). Figure 8 also shows a comparison between a DSM produced using a slice by slice unwrapping technique and a DSM produced using the method described in this paper. A gamma comparison at 3%/3 px shows a 96% agreement. Visual comparisons of dose maps with various dimensions show that a  $30 \times 30$  pixel dose map provides a sufficient resolution to view features of interest.

Lookup tables were created to provide dimensions of each pixel by calculating the distances to the next circumferential point and to the circumferential point in the next slice in order

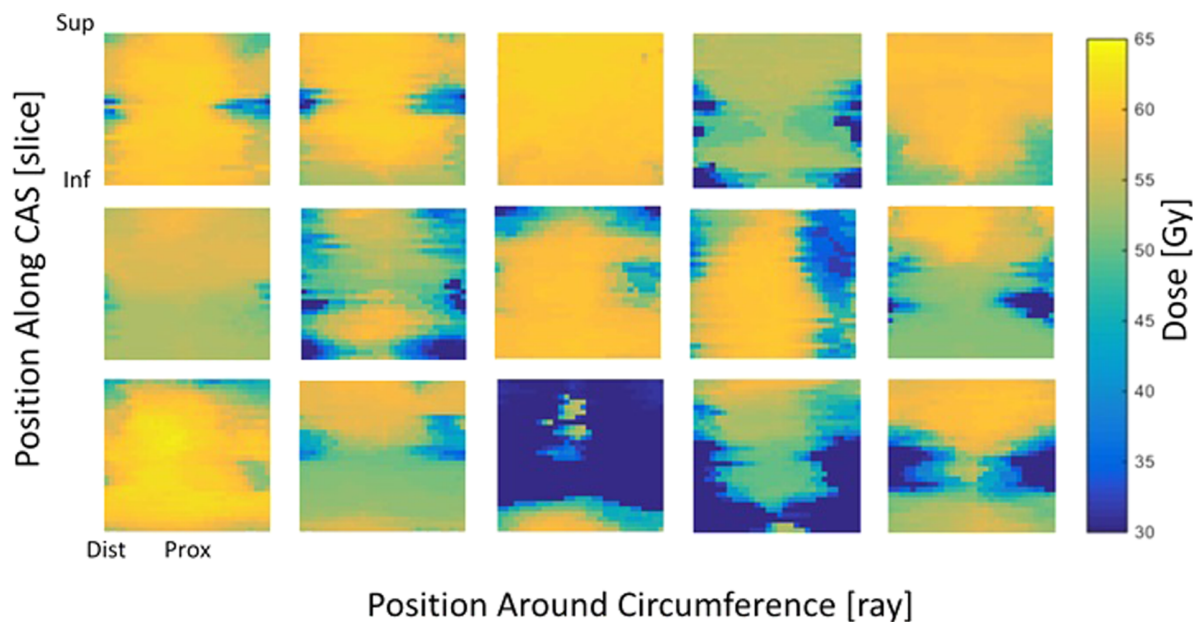


FIG. 7. Dose surface map for 15 unwrapped duodena with different dose distributions. The  $x$  and  $y$  axis labels are for each individual DSM. In the  $y$ -direction, each map comprises of the slices through the duodenum from superior (top) to inferior (bottom). In the  $x$ -direction, each map comprises of the surface points at each slice unwrapped from the point distal to the PTV so the center of each DSM is the point on the circumference most proximal to the PTV.

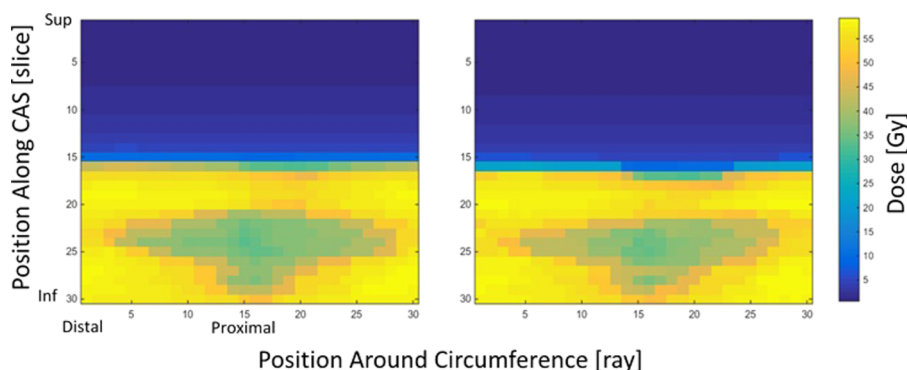


FIG. 8. Dose surface map for an esophagus unwrapped slice-by-slice (left) and using the method described in this paper (right). The  $y$ -direction comprises of the slices through the duodenum from superior (top) to inferior (bottom). The  $x$ -direction comprises of the surface points at each slice unwrapped from the point distal to the PTV so the center of each DSM is the point on the circumference most proximal to the PTV.

to extract absolute feature size. The lookup table is specific to each duodenum, and is in the form of a  $30 \times 30$  matrix where each cell contains the  $x$  and  $y$  dimensions of the corresponding pixel on the dose surface map. Averages, instead of individual pixel size calculations, were found to be unsuitable due to the range of variations (up to 6 mm in one dataset) between pixels. These variations are seen due to the orientation of slices around areas of high curvature.

### 3.B. Robustness

#### 3.B.1. Slice selection robustness

Different ways of uniformly sampling the 200 central axis spline points were compared and the gamma analysis results show very similar dose maps (Table II). First, a reference DSM was chosen where every six points between CAS points 14 and 188 were selected (i.e., 14, 20, 26... 182, 188). There was no overlap in this selection. A shift was introduced and two further slice selections with no overlap were created using every six slices between 10 and 184 (Shift 1) and 18–192 (Shift 2). The 3%/3 px gamma results showed there is nearly no difference in dose maps based on starting slice.

The selection of the reference dose-surface map is arbitrary and is not supposed to represent a gold standard. Since the unwrapping of the duodenum has never been done before, there is no gold standard with which to compare this method. The comparison to a reference DSM, however, still shows the robustness of the method to variations in slice selection.

Additionally, the reference DSM (14–188 every 6 points) with no overlap was compared to a DSM with the same

slice selection (14–188 every 6) but with overlapping slices (Overlap). This was done for the three patients by creating an additional central axis spline for testing purposes which resulted in overlap. In these cases, the gamma is reduced to below the accepted threshold of 95% in two out of the three duodena (91%, 100%, 52%).

#### 3.B.2. Overlap fix (polygon) robustness

In some cases with overlap, 30 sided planar polygons are replaced by 30 sided nonplanar polygons. The validity of using nonplanar polygons instead of flat polygons in areas of overlap was tested by replacing flat polygons with nonplanar polygons in two duodena that had no overlap. Planes were replaced in two straight edges of the duodenum ( $S1$ ,  $S2$ ) and one bend ( $B$ ). The DSMs produced by replacing three and five slices were compared to the original nonoverlapping plane DSMs and were found to be very similar (Table III).

## 4. DISCUSSION

### 4.A. Dose-surface maps

To our knowledge, this paper is the first to present 2D dose-surface maps of the duodenum and does so from clinical trial data. This is the first description of a new methodology for creating DSMs which generates a new coordinate system, defined as the position along the central axis spline, which overcomes the problems of the simple transaxial CT slice approach. This method has been successfully demonstrated,

TABLE II. Slice selection robustness. 3%/3 px gamma results comparing a reference selection (every six points from 14 to 188 with no overlap) for three patients to Shift 1 (every six from 10 to 184 with no overlap), Shift 2 (every six from 18 to 192 with no overlap), and Overlap (every six from 14 to 188 with overlap).

	Shift 1 (%)	Shift 2 (%)	Overlap (%)
Duodenum 1	99	99	91
Duodenum 2	100	100	100
Duodenum 3	100	100	52

TABLE III. Robustness (gamma 3%/3 px) of replacing 3 (3) or 5 (5) planes with 30 sided polygons in two straight sections of the duodenum ( $S1$ ,  $S2$ ) and one bend ( $B$ ) for two datasets (Duodenum 1, Duodenum 3).

	Duodenum 1 (%)	Duodenum 3 (%)
$S1$ (3)	100	100
$S2$ (3)	100	100
$B$ (3)	100	100
$S1$ (5)	99	100
$S2$ (5)	100	100
$B$ (5)	100	100



is robust, requires minimal human interaction, and has been shown to be generalizable.

The panel of DSMs in Fig. 7 shows a large variation in dose distribution for the 15 duodena. Even though each patient was treated to the same prescription, the different tumor locations and patient anatomy resulted in very different dose distributions.

In the more complex cases where overlap cannot be completely overcome using just the central axis spline, nonplanar polygons between fixed planar polygons are used to evenly and meaningfully sample the entire organ. This technique has only been required in one duodenal case out of fifteen duodena so far. The robustness of using nonplanar polygons instead of flat polygons has been shown to have very little effect on the resulting dose-surface map when there is no overlap in the slices. Therefore, the DSMs produced using the overlap fix method described when the overlap is not overcome through the initial central axis spline selection provide a valid description of the surface dose.

The problem of overlapping planes when unwrapping organs was acknowledged in work unwrapping the rectum<sup>23</sup> where this was avoided but not quantified. In other work it has been ignored. In virtual colonography overlapping planes are avoided by bending the rays cast from the centre line. In this paper we present an alternative solution which keeps the rays linear but moves the central axis. We have also quantified the effect of overlapping planes on dose surface maps for the first time.

Due to the complex shape of the duodenal surface, the DSMs present a relative space that can be converted to absolute size. The curvature of the organ is such that the distances between pixels on the dose map vary. For this reason, a pixel-specific lookup table was created to convert from pixels to surface area. Therefore, extracted features from the DSM can either be described in absolute size or in relative position along the organ.

Compared to previous methods applied to other organs,<sup>21,23,24</sup> which can only be used when the CT transaxial slices can be unwrapped individually, this approach allows for the unwrapping of any tubular organ and also provides a mechanism for checking and fixing overlapping planes. However, this thorough approach to a generalizable nonoverlapping tubular unwrapping technique also leads to an element of human interaction in the selection of start and end points.

Validation of this method is a multifaceted problem. There may be a need to validate the unwrapping geometry but also, and we believe more importantly, there will be a need to validate the predictive model that can now be built using spatial information from the DSMs against clinical toxicity data. A means of validation of the unwrapping geometry that is currently being explored is the use of a post-operative pathological sample which can be physically cut open and unwrapped. There is currently no commercial software or alternative method which can produce DSMs of the duodenum against which we could validate our approach.

Future use of the dose-surface map could include better planning constraints, toxicity models, and daily maps to check whether the delivered dose matches the planned dose.

## 4.B. Robustness

Although dose-surface maps have been produced for other organs, their robustness has not been quantified. A preliminary study was undertaken to investigate the effect of different sampling techniques, overlap, and different length and curvature penalties on the dose map.

The most spatially meaningful sampling of the organ requires uniform slice selection throughout the duodenum and that the angular slices do not overlap. The robustness of the dose-surface maps to where these slices start and end shows that there are only very small differences ( $\gamma$  3%/3 px > 99%). These differences increase when looking at the effect of overlapping planes where  $\gamma$  (3%/3 px) can be reduced to as low as 52% compared to a nonoverlapping selection, highlighting the need for a solution to the plane overlap problem.

The effect of overlapping planes on the dose surface map was expected because each overlapping plane results in a spatially meaningless row on the dose-surface map. The effect of overlap varied for the three duodena studied. On one duodenum, overlap had almost no effect whereas on another the  $\gamma$  3%/3 px between the nonoverlap DSM and the overlap DSM was 52%. This range is also expected as overlap can mean just the edge of two planes overlapping as seen in Fig. 5 or it can mean a few planes overlapping with a few planes. In areas of high curvature this can lead to sampling from an area of the surface that is very distant to the area intended.

This suggests that the overlapping problem causes the most change to the DSMs and needs to be considered in future work.

In areas of high curvature or complex geometry, the racecar algorithm requires a minimum of one voxel separation between two outside surfaces to ensure that the anatomy of the organ is honored and the path does not “jump” between two areas. However, in reality such curvature does not occur in the duodenum. Additionally, such curvature would present a greater obstacle at the contouring stage. If such a case would need to be solved, an increase in grid resolution using interpolation could be added to solve such edge cases.

## 5. CONCLUSIONS

Dose-surface maps produced provide previously unexamined information on the spatial dose distribution in the duodenum which can now be explored to create models that may improve duodenal toxicity predictions. When unwrapping 3D hollow organs to a 2D dose surface-map, care must be taken to ensure slices do not overlap. Spatial dose metrics will be extracted from the DSMs and the best predictors for duodenal toxicity will be identified.

## ACKNOWLEDGMENTS

Alon Witztum is supported by an MRC/Gray Institute DPhil Studentship. Samantha Warren and Mike Partridge are supported by CRUK Grant No. C5255/A15935. Maria Hawkins received an MRC Fellowship MC\_PC\_12001/2. Additional data and materials may be requested from Professor Maria Hawkins.



## CONFLICT OF INTEREST DISCLOSURE

The authors have no COI to report.

<sup>a)</sup>Electronic mail: alon.witztum@oncology.ox.ac.uk

- <sup>1</sup>Cancer Research UK, "Pancreatic cancer survival statistics," <http://www.cancerresearchuk.org/health-professional/cancer-statistics/statistics-by-cancer-type/pancreatic-cancer/survival>, 2015, retrieved 17 August 2016.
- <sup>2</sup>B. Gudjonsson, "Cancer of the pancreas: 50 years of surgery," *Cancer* **60**, 2284–2303 (1987).
- <sup>3</sup>K. A. Goodman and C. Hajj, "Role of radiation therapy in the management of pancreatic cancer," *J. Surg. Oncol.* **107**, 86–96 (2013).
- <sup>4</sup>J. D. Murphy, S. Adusumilli, K. A. Griffith, M. E. Ray, M. M. Zalupski, T. S. Lawrence, and E. Ben-Josef, "Full-dose gemcitabine and concurrent radiotherapy for unresectable pancreatic cancer," *Int. J. Radiat. Oncol., Biol., Phys.* **68**, 801–808 (2007).
- <sup>5</sup>P. Kelly, P. Das, C. C. Pinnix, S. Beddar, T. Briere, M. Pham, S. Krishnan, M. E. Delclos, and C. H. Crane, "Duodenal toxicity after fractionated chemoradiation for unresectable pancreatic cancer," *Int. J. Radiat. Oncol., Biol., Phys.* **85**, e143–e149 (2013).
- <sup>6</sup>B. Chaffert, F. Mornex, F. Bonnetain, P. Rougier, C. Mariette, O. Bouché, J. F. Bosset, T. Aparicio, L. Mineur, A. Azzedine, P. Hammel, J. Butel, N. Stremisdoerfer, P. Maingon, and L. Bedenne, "Phase III trial comparing intensive induction chemoradiotherapy (60 Gy, infusional 5-FU and intermittent cisplatin) followed by maintenance gemcitabine with gemcitabine alone for locally advanced unresectable pancreatic cancer. Definitive results of the 2," *Ann. Oncol.* **19**, 1592–1599 (2008).
- <sup>7</sup>H. M. Ceha, G. van Tienhoven, D. J. Gouma, C. H. Veenhof, C. J. Schneider, E. A. Rauws, S. S. Phoa, and D. González González, "Feasibility and efficacy of high dose conformal radiotherapy for patients with locally advanced pancreatic carcinoma," *Cancer* **89**, 2222–2229 (2000).
- <sup>8</sup>C. G. Willett, C. F. D. Castillo, H. A. Shih, S. Goldberg, P. Biggs, J. W. Clark, G. Lauwers, D. P. Ryan, A. X. Zhu, and A. L. Warshaw, "Long-term results of intraoperative electron beam irradiation (IOERT) for patients with unresectable pancreatic cancer," *Ann. Surg.* **241**, 295–299 (2005).
- <sup>9</sup>J. D. Murphy, C. Christman-Skieller, J. Kim, S. Dieterich, D. T. Chang, and A. C. A. Koong, "Dosimetric model of duodenal toxicity after stereotactic body radiotherapy for pancreatic cancer," *Int. J. Radiat. Oncol., Biol., Phys.* **78**, 1420–1426 (2010).
- <sup>10</sup>T. B. Brunner, U. Nestle, A.-L. Grosu, and M. Partridge, "SBRT in pancreatic cancer: What is the therapeutic window?," *Radiother. Oncol.* **114**, 109–116 (2015).
- <sup>11</sup>S. Krishnan, A. S. Chadha, Y. Suh, P. Das, B. D. Minsky, U. Mahmood, M. E. Delclos, G. O. Sawakuchi, S. Beddar, M. H. Katz, J. B. Fleming, M. M. Javle, G. R. Varadhachary, R. A. Wolff, and C. H. Crane, "Focal radiotherapy dose escalation improves overall survival in locally advanced pancreatic cancer patients receiving induction chemotherapy and consolidative chemoradiation," *Int. J. Radiat. Oncol., Biol., Phys.* **94**, 755–765 (2015).
- <sup>12</sup>G. M. Cattaneo, P. Passoni, B. Longobardi, N. Slim, M. Reni, S. Cereda, N. di Muzio, and R. Calandrino, "Dosimetric and clinical predictors of toxicity following combined chemotherapy and moderately hypofractionated rotational radiotherapy of locally advanced pancreatic adenocarcinoma," *Radiother. Oncol.* **108**, 66–71 (2013).
- <sup>13</sup>J. Huang, J. M. Robertson, H. Ye, J. Margolis, L. Nadeau, and D. Yan, "Dose-volume analysis of predictors for gastrointestinal toxicity after concurrent full-dose gemcitabine and radiotherapy for locally advanced pancreatic adenocarcinoma," *Int. J. Radiat. Oncol., Biol., Phys.* **83**, 1120–1125 (2012).
- <sup>14</sup>A. Nakamura, K. Shibuya, Y. Matsuo, M. Nakamura, T. Shiinoki, T. Mizowaki, and M. Hiraoka, "Analysis of dosimetric parameters associated with acute gastrointestinal toxicity and upper gastrointestinal bleeding in locally advanced pancreatic cancer patients treated with gemcitabine-based concurrent chemoradiotherapy," *Int. J. Radiat. Oncol., Biol., Phys.* **84**, 369–375 (2012).
- <sup>15</sup>S. Li, A. Boyer, Y. Lu, and G. T. Chen, "Analysis of the dose-surface histogram and dose-wall histogram for the rectum and bladder," *Med. Phys.* **24**, 1107–1116 (1997).
- <sup>16</sup>R. I. MacKay, J. H. Hendry, C. J. Moore, P. C. Williams, and G. Read, "Predicting late rectal complications following prostate conformal radiotherapy using biologically effective doses and normalized dose-surface histograms," *Br. J. Radiol.* **70**, 517–526 (1997).
- <sup>17</sup>J. D. Fenwick, V. S. Khoo, A. E. Nahum, B. Sanchez-Nieto, and D. P. Dearnaley, "Correlations between dose-surface histograms and the incidence of long-term rectal bleeding following conformal or conventional radiotherapy treatment of prostate cancer," *Int. J. Radiat. Oncol., Biol., Phys.* **49**, 473–480 (2001).
- <sup>18</sup>L. B. Marks, E. D. Yorke, A. Jackson, R. K. T. Haken, L. S. Constine, A. Eisbruch, S. M. Bentzen, J. Nam, and J. O. Deasy, "Use of normal tissue complication probability models in the clinic," *Int. J. Radiat. Oncol., Biol., Phys.* **76**, S10–S19 (2010).
- <sup>19</sup>R. Munbodh, A. Jackson, J. Bauer, C. R. Schmidlein, and M. J. Zelefsky, "Dosimetric and anatomic indicators of late rectal toxicity after high-dose intensity modulated radiation therapy for prostate cancer," *Med. Phys.* **35**, 2137–2150 (2008).
- <sup>20</sup>F. Buettner, S. L. Gulliford, S. Webb, M. R. Sydes, D. P. Dearnaley, and M. Partridge, "Assessing correlations between the spatial distribution of the dose to the rectal wall and late rectal toxicity after prostate radiotherapy: An analysis of data from the MRC RT01 trial (ISRCTN 47772397)," *Phys. Med. Biol.* **54**, 6535–6548 (2009).
- <sup>21</sup>S. M. Zhou, L. B. Marks, G. S. Tracton, G. S. Sibley, K. L. Light, P. D. Maguire, and M. S. Anscher, "A new three-dimensional dose distribution reduction scheme for tubular organs," *Med. Phys.* **27**, 1727–1731 (2000).
- <sup>22</sup>F. Buettner, S. L. Gulliford, S. Webb, and M. Partridge, "Using dose-surface maps to predict radiation-induced rectal bleeding: A neural network approach," *Phys. Med. Biol.* **54**, 5139–5153 (2009).
- <sup>23</sup>M. S. Hoogeman, M. van Herk, J. de Bois, P. Muller-Timmermans, P. C. M. Koper, and J. V. Lebesque, "Quantification of local rectal wall displacements by virtual rectum unfolding," *Radiother. Oncol.* **70**, 21–30 (2004).
- <sup>24</sup>J. E. Scaife, S. J. Thomas, K. Harrison, M. Romanchikova, M. P. F. Sutcliffe, J. R. Forman, A. M. Bates, R. Jena, M. A. Parker, and N. G. Burnet, "Accumulated dose to the rectum, measured using dose-volume histograms and dose-surface maps, is different from planned dose in all patients treated with radiotherapy for prostate cancer," *Br. J. Radiol.* **88**, 20150243 (2015).
- <sup>25</sup>S. Haker, S. Angenent, A. Tannenbaum, and R. Kikinis, "Nondistorting flattening maps and the 3-D visualization of colon CT images," *IEEE Trans. Med. Imaging* **19**, 665–670 (2000).
- <sup>26</sup>S. L. Tucker, M. Zhang, L. Dong, R. Mohan, D. Kuban, and H. D. Thames, "Cluster model analysis of late rectal bleeding after IMRT of prostate cancer: A case-control study," *Int. J. Radiat. Oncol., Biol., Phys.* **64**, 1255–1264 (2006).
- <sup>27</sup>A. V. Vilanova Bartoli, R. Wegenkittl, A. König, and E. Groller, "Nonlinear virtual colon unfolding," in *Proceedings Visualization, 2001. VIS '01* (IEEE, San Diego, CA, 2001), pp. 411–419.
- <sup>28</sup>G. Wang, E. G. McFarland, B. P. Brown, and M. W. Vannier, "GI tract unraveling with curved cross sections," *IEEE Trans. Med. Imaging* **17**, 318–322 (1998).
- <sup>29</sup>J. O. Deasy, A. I. Blanco, and V. H. Clark, "CERR: A computational environment for radiotherapy research," *Med. Phys.* **30**, 979–985 (2003).
- <sup>30</sup>J. Ulén, P. Strandmark, and F. Kahl, "Shortest paths with higher-order regularization," *IEEE Trans. Pattern Anal. Mach. Intell.* **37**, 2588–2600 (2015).
- <sup>31</sup>J. D. Hobby, "Smooth, easy to compute interpolating splines," *Discrete Comput. Geom.* **1**, 123–140 (1986).
- <sup>32</sup>D. A. Low, W. B. Harms, S. Mutic, and J. A. Purdy, "A technique for the quantitative evaluation of dose distributions," *Med. Phys.* **25**, 656–661 (1998).